

# Piezoelectric Negative Capacitance

*Justin Wong  
Sayeef Salahuddin*



Electrical Engineering and Computer Sciences  
University of California at Berkeley

Technical Report No. UCB/EECS-2015-57

<http://www.eecs.berkeley.edu/Pubs/TechRpts/2015/EECS-2015-57.html>

May 11, 2015

Copyright © 2015, by the author(s).  
All rights reserved.

Permission to make digital or hard copies of all or part of this work for personal or classroom use is granted without fee provided that copies are not made or distributed for profit or commercial advantage and that copies bear this notice and the full citation on the first page. To copy otherwise, to republish, to post on servers or to redistribute to lists, requires prior specific permission.

---

# Piezoelectric Negative Capacitance

Justin C. Wong

---

## Research Project

Submitted to the Department of Electrical Engineering and Computer Sciences, University of California at Berkeley, in partial satisfaction of the requirements for the degree of **Master of Science, Plan II.**

Approval for the Report and Comprehensive Examination:

### Committee:

---

Sayeef Salahuddin  
Research Advisor

---

Date

\* \* \* \* \*

---

Jeffrey Bokor  
Second Reader

---

Date

## **Abstract**

A thermodynamic model was constructed to analyze the negative capacitance effect in the presence of piezoelectricity. The model demonstrated that while piezoelectricity can lead to negative capacitance in principle, it is not strong enough in practice due to the unphysical amounts of charge and strain required. The inclusion of higher-order electromechanical coupling such as electrostriction can make the negative capacitance region accessible at a lower amount of charge. However, the required strains are still unphysical on the order of tens of percent. Furthermore, the material must possess a negative electrostriction coefficient, or else the negative capacitance effect will be suppressed by positive electrostriction. Most commonly used oxides, however, possess positive electrostriction coefficients. Finally, piezoelectricity, electrostriction, and ferroelectricity were analyzed together to show that a negative capacitance effect occurs but due to ferroelectricity and not piezoelectricity. The model ultimately demonstrates that for all practical purposes, pure electromechanical coupling is not strong enough to provide a negative capacitance effect.

## Acknowledgements

I started taking piano lessons as a child under the tutelage of a concert pianist after playing “Hall of the Mountain King” by ear. I quit a few months later. By middle school, I was trying to build a wooden boat to sail to a deserted island and live out the rest of my days eating coconuts (my parents did not support this particular expedition unfortunately). In high school, I scoffed at the idea of PhD, and thought UC Berkeley and electrical engineering were boring...and now here I am. Mom, I don’t know how you put up with all the crazy ideas I come up with that must seem oh so strange to you, and I don’t know where I’ll end up next; but thanks for always coming along for the ride. By the way, I’ve been thinking lately that we should move back to Hawaii and open up a pineapple plantation.

Now with respect to the research that went into this report, I first want to thank my advisor, Professor Sayeef Salahuddin, for guiding and supporting me these past couple years. I feel blessed to have found such a laid-back advisor that encourages me to explore my own research interests rather than forcing me to complete cookie-cutter project after project. I look forward to solving more scientific mysteries with you.

Next, I want to thank Dr. Sapan Agarwal. We first met when I blew his mind with the solution to the “100 prisoners” problem. Thank you, Sapan, for always participating in productive late night arguments discussions with me about ferroelectrics, negative capacitance, and what made “free energy” *free* (I’ll let you know when I figure that one out).

Last but not least, I want to thank Professor Jeffrey Bokor for agreeing to be the second reader for my master’s report. Were it not for him, I would not be able to receive my master’s degree. Thank you, Professor Bokor.

# Contents

<b>1</b>	<b>Introduction</b>	<b>2</b>
1.1	Subthreshold Swing . . . . .	2
1.2	Ferroelectric Negative Capacitance . . . . .	3
1.3	Evidence of Piezoelectric Negative Capacitance . . . . .	5
<b>2</b>	<b>Background</b>	<b>6</b>
2.1	Negative Capacitance . . . . .	6
2.2	Piezoelectricity . . . . .	7
2.3	Electrostriction . . . . .	8
2.4	Maxwell Stress . . . . .	9
2.5	Thermodynamics of Electroelastic Materials . . . . .	10
<b>3</b>	<b>Thermodynamic Model</b>	<b>12</b>
3.1	Setup . . . . .	12
3.2	Model and Simulation . . . . .	13
<b>4</b>	<b>Results</b>	<b>14</b>
4.1	Piezoelectric Negative Capacitance . . . . .	14
4.2	Incorporating Electrostriction . . . . .	16
4.3	Tuning Electromechanical Negative Capacitance . . . . .	18
4.4	Negative Capacitance in PZT . . . . .	20
<b>5</b>	<b>Conclusion</b>	<b>22</b>
	<b>References</b>	<b>23</b>

# 1

## Introduction

Conventional scaling in modern MOSFETs has become limited by nonscaling effects due to scale-independent material parameters and fundamental limits in the physics utilized. Boltzmann statistics, for example, imposes a thermal voltage  $\frac{k_B T}{q}$  that does not change with scale. This places a fundamental lower limit on subthreshold swing, which limits threshold voltage scaling and, subsequently, power supply voltage scaling. The net result is smaller devices with relatively higher off-state leakage current and static power consumption—among other performance-related issues—with each generation of scaling.

This problem can be alleviated by following one of a number of approaches. For example, devices that do not switch via Boltzmann statistics such as the tunnel field-effect transistor (TFET) do not suffer from the same limitations as conventional MOSFETs due to different physics utilized. Such devices, however, have their own problems that must be taken into consideration [1]. Alternatively, *negative capacitance* has emerged as a promising solution for achieving steep subthreshold slope without foregoing Boltzmann statistics altogether. This works by effectively amplifying the gate voltage output at the semiconductor surface and can be better understood by revisiting the concept of subthreshold swing from basic device physics.

### 1.1 Subthreshold Swing

*Subthreshold swing*  $S$  is the change in gate voltage  $V_g$  needed to change the drain current  $I_d$  of a transistor by a single decade. Mathematically, this can be expressed as

$$S = \frac{\partial V_g}{\partial \log_{10}(I_d)} = \underbrace{\frac{\partial V_g}{\partial \psi_s}}_m \underbrace{\frac{\partial \psi_s}{\partial \log_{10}(I_d)}}_{60 \text{ mV/decade at room temperature}} \quad (1.1)$$

where  $\psi_s$  is the semiconductor surface potential, and  $m$  is the *body factor*. The body factor represents the capacitive coupling between the gate and channel and can be expressed using a simple capacitor model (Figure 1.1) as

$$m = 1 + \frac{C_s}{C_{\text{ins}}} \quad (1.2)$$

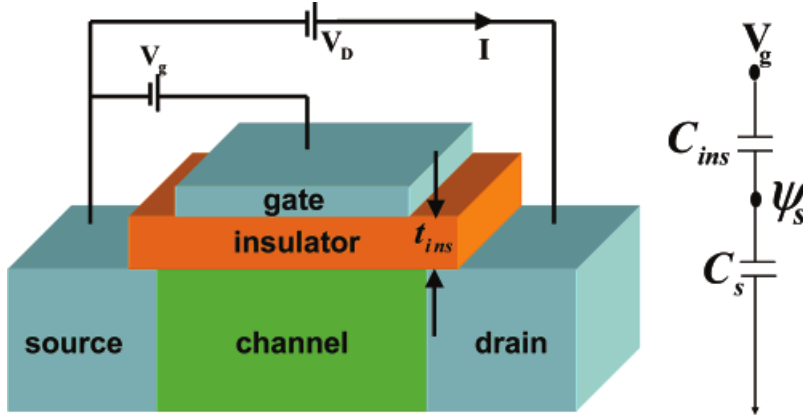


**Figure 1.1.** Schematic of a simple MOSFET with corresponding capacitor model.  $C_s$  includes the depletion, channel-drain, and channel-source capacitances [2].

where  $C_s$  is the semiconductor capacitance, and  $C_{ins}$  is the effective gate insulator capacitance. Since capacitance is normally positive,  $m$  is typically assumed to have a lower limit of one. Thus, if we assume perfect capacitive coupling between the gate and the channel (i.e.  $m = 1$ ), then from Equation 1.1 we can see that subthreshold swing has a lower limit of 60 mV/decade at room temperature. **Notice, however, that if it were possible to make one of the capacitances in Equation 1.2 negative, then we could reduce the body factor below its ideal limit of one.**

## 1.2 Ferroelectric Negative Capacitance

In 2008, Salahuddin et al. showed that by changing the gate oxide of a MOSFET to a ferroelectric material, the effective insulator capacitance becomes *negative* [2]. As a result, the body factor *decreases* below its ideal limit of one, consequently reducing subthreshold swing below the “Boltzmann limit” of 60 mV/decade. Since this novel idea was proposed, much research has been conducted using ferroelectric insulators in attempts to experimentally observe negative capacitance and subthreshold swing reduction. In 2010, for example, Rusu et al. observed subthreshold swings below the Boltzmann limit for portions of the switching in metal-ferroelectric-metal-oxide-semiconductor (MFeMOS) FETs as shown in Figure 1.2:

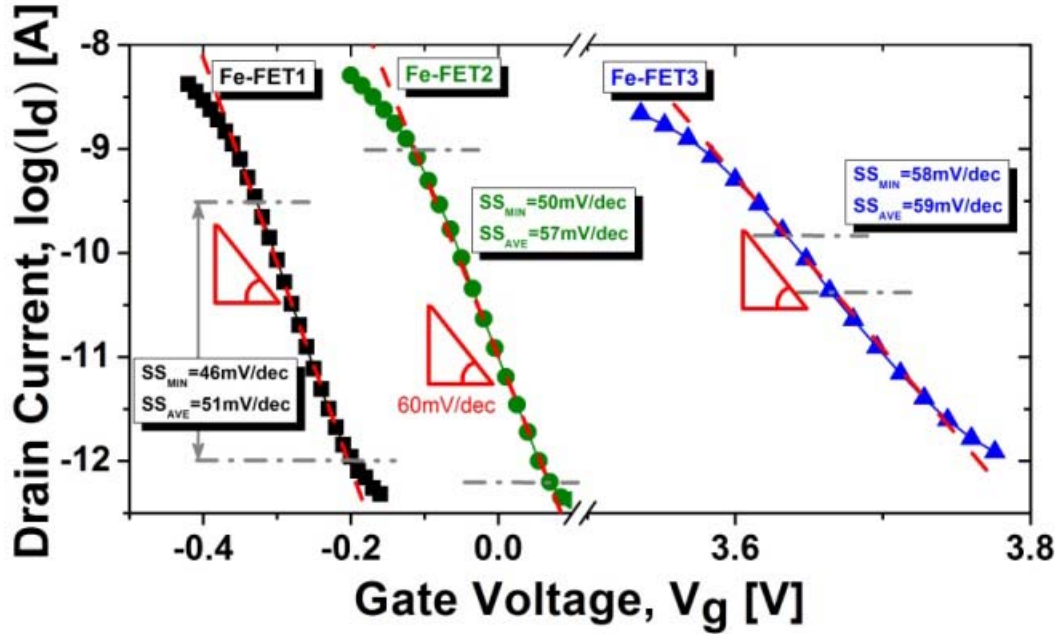


**Figure 1.2.** Experimental evidence of sub-60 mV/decade subthreshold swing in MFeMOSFETs due to ferroelectric negative capacitance [3].

Clearly, we can see sub-60 mV/decade minimum and average subthreshold swings for part of the switching in all three devices shown.

In 2011, Khan et al. showed the first proof-of-concept experimental evidence of negative capacitance in ferroelectric-dielectric (FE-DE) heterostructures shown in Figure 1.3:

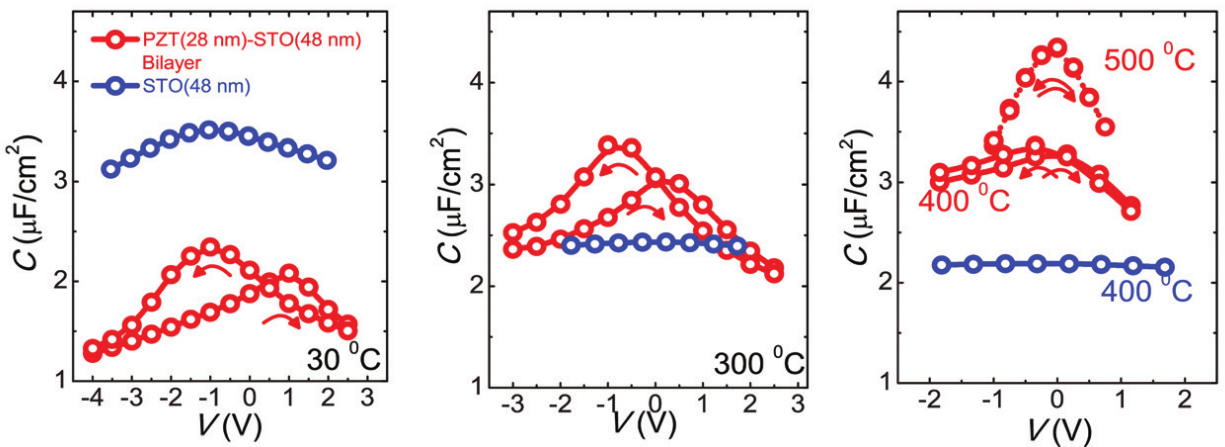


**Figure 1.3.** Proof-of-concept experimental evidence of negative capacitance in FE-DE heterostructures. Changing the temperature tunes the strength of the ferroelectric negative capacitance [4].

The red lines correspond to the C-V curves of 76 nm FE-DE heterostructures while the blue lines correspond to the C-V curves of 48 nm DE homostructures. From basic physics, we expect the thicker heterostructure to have a smaller capacitance than the thinner homostructure. When examining the figure, however, we can see a clear capacitance *enhancement* in the thicker FE-DE

heterostructure when the temperature is sufficiently high for strong enough ferroelectricity to occur. This capacitance enhancement for a thicker gate stack is a signature of negative capacitance.

There have also been many other important research developments for negative capacitance (see References [5–9]), but they have all focused on *ferroelectric* negative capacitance. Ferroelectrics have their own problems with respect to fabrication and integration with standard silicon processes [4]. Thus, it would be useful to find another material that also exhibits negative capacitance but is easier to integrate with existing processes. *Piezoelectric* materials, for example, are more numerous than ferroelectrics due to fewer crystal symmetry requirements [10] and have fewer integration challenges.

### 1.3 Evidence of Piezoelectric Negative Capacitance

At the 2013 IEEE International Electron Devices Meeting (IEDM), Then et al. showed that subthreshold swing was reduced below the Boltzmann limit to 40 mV/decade when an ultrathin piezoelectric AlInN layer was added to the gate stack of a MOS high electron mobility transistor (MOS-HEMT). C-V curves before and after adding the piezoelectric layer are indicated by the dashed and solid lines respectively in the left graph of Figure 1.4:

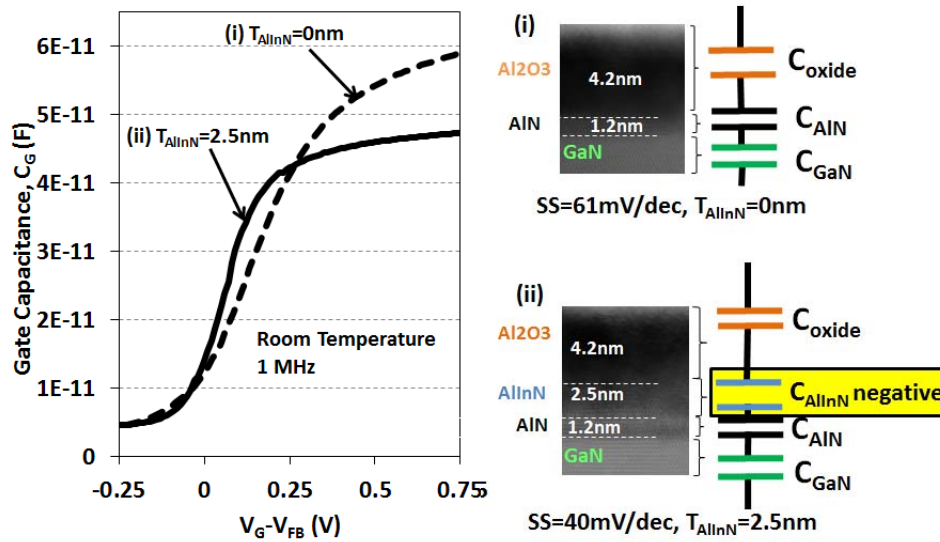


**Figure 1.4.** MOS-HEMT C-V curves for two different gate stacks [11]. (i) A subthreshold swing of 61 mV/decade was observed for this particular gate stack. (ii) An ultrathin 2.5 nm piezoelectric AlInN layer was added to the gate stack, and the observed subthreshold swing decreased below the Boltzmann limit to 40 mV/decade during switching.

The MOS-HEMT with the piezoelectric layer should have a smaller capacitance due to a thicker gate stack, and we can observe this in the above graph for gate voltages above the threshold voltage. However, during switching, we see that the MOS-HEMT with the piezoelectric layer possessed greater capacitance than that of the MOS-HEMT with the thinner gate stack. As mentioned in the previous section, this capacitance enhancement is a signature of negative capacitance. This led many to ask the following question: **can piezoelectricity lead to a negative capacitance effect that has been overlooked thus far?**

# 2

## Background

### 2.1 Negative Capacitance

In order to study *piezoelectric* negative capacitance, we first need to understand general negative capacitance at a more fundamental level. As it turns out, negative capacitance can be understood in terms of simple positive feedback [2] as shown in Figure 2.1:

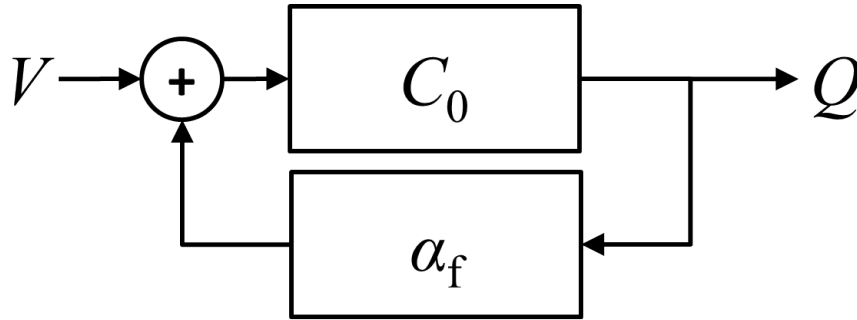


Figure 2.1. A simple capacitive system with a feedback loop.

Here we have a simple capacitive system  $C_0$  with a feedback loop characterized by a feedback factor  $\alpha_f$ . A quick analysis reveals that the effective charge  $Q$  stored in the system for an applied voltage  $V$  is given by

$$Q = \underbrace{\left( \frac{C_0}{1 - \alpha_f C_0} \right)}_{C_{\text{ins}}} V \quad (2.1)$$

where  $C_{\text{ins}}$  is the effective capacitance of the overall system. Notice that if the feedback is strong enough such that  $\alpha_f C_0 > 1$ , then the effective capacitance actually becomes *negative*. The exact feedback mechanism is unimportant as long as it is sufficiently strong; if the feedback is not strong enough, then the effective capacitance will only become non-linear rather than negative. **Thus, in order for piezoelectricity to provide a negative capacitance effect, there must exist a sufficiently strong positive feedback mechanism that exploits piezoelectricity.**

## 2.2 Piezoelectricity

Piezoelectricity can be understood as *linear electromechanical coupling*, or a linear coupling that transforms mechanical energy into electrical energy and vice versa. For example, mechanically stressing a piezoelectric material will electrically polarize the material. Conversely, applying an electric field across a piezoelectric material will mechanically strain the material. These effects are termed the *direct piezoelectric effect* and *converse piezoelectric effect* respectively.

In order to understand how these effects work, we can consider the simple 1-D spring model shown in Figure 2.2a:

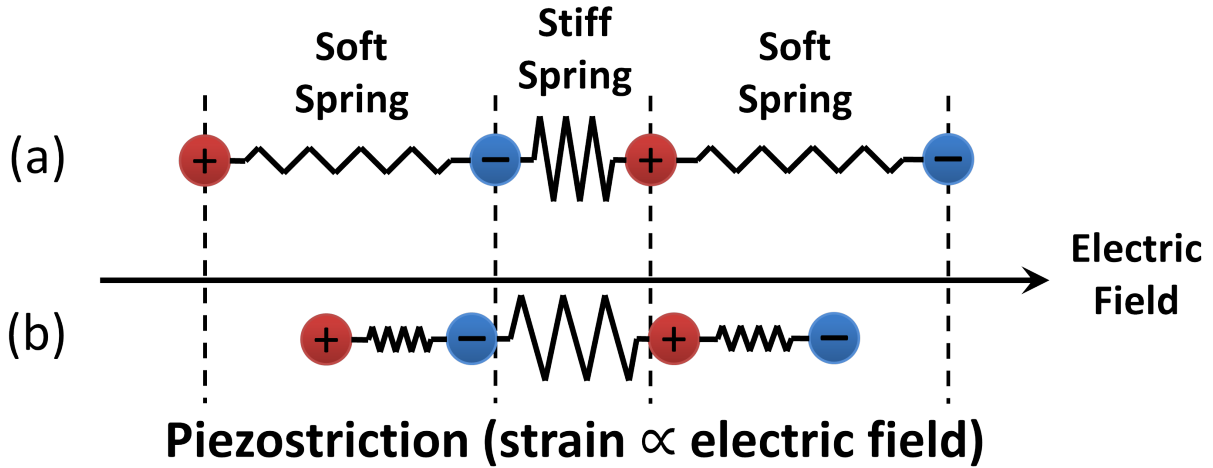


**Figure 2.2.** (a) 1-D spring model of a piezoelectric crystal. (b) Applying an electric field results in a net strain due to the particular symmetry of the crystal. [12]

Notice that the model possesses both stiff springs and soft springs. This reflects the particular non-centrosymmetric crystal structure required for a material to exhibit piezoelectricity [10]. Due to this structure, applying an electric field in the direction depicted in Figure 2.2b compressively strains the soft springs more than the stiff springs can elongate. Consequently, the material exhibits a net compressive strain. Since piezoelectricity is an asymmetric effect, reversing the direction of the electric field will also change the net strain from compressive to tensile. Although we only explained the converse piezoelectric effect here, it is trivial to demonstrate the direct piezoelectric effect using the same model by replacing the electrostatic force with a mechanical stress.

The piezoelectric effect can be expressed mathematically using constitutive equations such as

$$\varepsilon_{ij} = s_{ijkl}\sigma_{kl} + d_{ijk}E_i \quad (2.2)$$

$$D_i = \epsilon_{ij}E_j + d_{ijk}\sigma_{jk} \quad (2.3)$$

where  $\sigma_{ij}$  and  $\varepsilon_{ij}$  and are the stress and strain tensors respectively;  $E_i$  and  $D_i$  are the electric field and electric displacement field respectively;  $s_{ijkl}$  is the elastic compliance tensor;  $d_{ijk}$  is the piezoelectric coefficient tensor; and  $\epsilon_{ij}$  is the dielectric permittivity tensor (do not confuse the “inverted-3” epsilon  $\varepsilon$  representing strain with the lunate epsilon  $\epsilon$  representing dielectric permittivity). Note that the above equations assume a linearly polarizable material. For non-linear materials such as

ferroelectrics, the electric displacement field must be rewritten as  $\epsilon_0 E_i + P_i$  where  $P_i$  represents polarization due to external electric fields, ferroelectricity, and piezoelectricity. This polarization is most easily determined by using an appropriately defined free energy that takes into account all of the necessary effects [13].

It is also important to note that Equations 2.2 and 2.3 are specifically the *strain-charge* form of the constitutive piezoelectric equations. There are three other forms that can be used depending on the control and response variables chosen from each pair of thermodynamic conjugate variables. For example, stress and strain are conjugate variables as well as electric field and electric displacement field. For every such conjugate pair, one variable can be experimentally controlled while the other variable is allowed to freely change in response. Thus, by choosing different control and response variables from each conjugate pair, four different sets of constitutive equations can be formed. This also highlights the fact that material constants such as elastic compliance and piezoelectric coefficient will differ based on the control and response variables used during measurement. For more information, please refer to References [14, 15].

## 2.3 Electrostriction

Since piezoelectricity is linear electromechanical coupling, it is only valid for “small” electric fields. For larger electric fields, higher-order electromechanical coupling known as *electrostriction* must be taken into account. To understand the difference between electrostriction and piezoelectricity, we can refer to the 1-D spring model shown in Figure 2.3a:

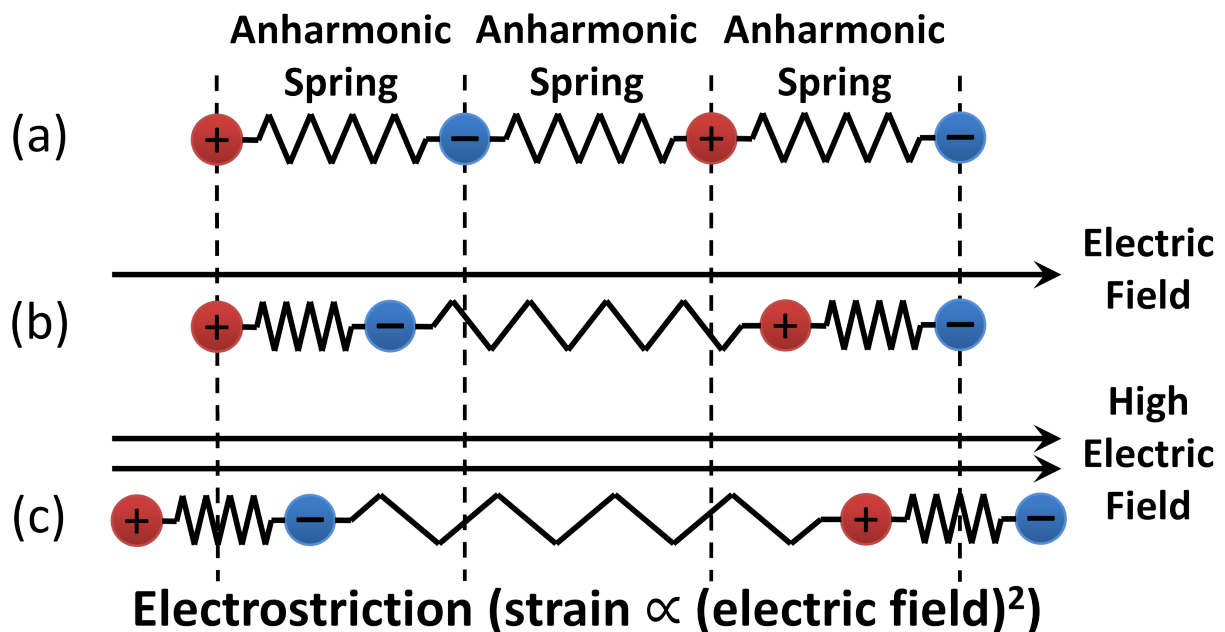


**Figure 2.3.** (a) A simple 1-D spring model of a dielectric. Note that all of the springs are identical. (b) When an electric field is applied, the overall crystal does not strain because all of the springs strain symmetrically to first order. (c) When a strong electric field is applied, the crystal exhibits a net tensile strain because the springs tend to stretch more easily than compress in this particular case. The strain is proportional to the electric field squared. [12]

Notice that all of the springs are identical but have their anharmonicities taken into account. This reflects the fact that electrostriction is present in all crystal classes and does not require particular symmetries [16]. The springs strain symmetrically for small strains, but may be easier to stretch than compress or vice versa for large strains due to the anharmonicity. Thus, when an electric field is applied across an ordinary dielectric as depicted in Figure 2.3b, the material does not exhibit net strain to first order. However, if the electric field strength is increased enough, then the anharmonicity of the springs becomes more prevalent as shown in Figure 2.3c. In this case, we assume that the springs tend to elongate more easily than compress for high strains, resulting in a net tensile strain that is roughly proportional to the electric field squared. This reflects the fact that **most materials expand under high electric fields** [12]. This also reveals that electrostriction is a symmetric effect; applying an equally strong electric field in the opposite direction will result in the same strain.

Mathematically, the strain due to electrostriction can be expressed as

$$\varepsilon_{ij} = M_{ijkl}E_kE_l + W_{ijklmn}E_kE_lE_mE_n + \dots \quad (2.4)$$

where  $M_{ijkl}$  and  $W_{ijklmn}$  are the second-order and fourth-order electrostriction coefficient tensors respectively. Since electrostriction is simply higher-order electromechanical coupling, it can be extended to as many even orders as applies for the material of interest. Most materials, however, experience dielectric breakdown before high enough electric fields can be reached to require fourth-order or higher electrostriction terms.

For ferroelectric materials, experimental results show that electrostriction is better modeled in terms of even orders of polarization [16]:

$$\varepsilon_{ij} = Q_{ijkl}P_kP_l + \dots \quad (2.5)$$

Note that  $Q_{ijkl}$  here is the electrostriction coefficient tensor and not electric charge. Unfortunately, this conflicting notation is standard. For linearly polarizable materials, the electrostriction coefficient tensors  $M_{ijkl}$  and  $Q_{ijkl}$  are easily relatable by equating corresponding orders of electrostriction [16]. Using second-order electrostriction as an example, we can setup the following equation:

$$M_{ijkl}E_kE_l = Q_{ijkl}P_kP_l \quad (2.6)$$

Either  $M_{ijkl}$  or  $Q_{ijkl}$  can be solved for in terms of the other.

## 2.4 Maxwell Stress

Consider a parallel-plate capacitor charged such that the plates have surface charge densities  $+\rho_s$  and  $-\rho_s$ . From Gauss's Law, the electric field  $E_{\text{plate}}$  produced by the positively charged plate is given by

$$E_{\text{plate}} = \frac{\rho_s}{2\epsilon} = \frac{E_{\text{total}}}{2} \quad (2.7)$$

where  $E_{\text{total}}$  is the total electric field between the plates. Thus, there is an attractive electrostatic stress  $\sigma_{\text{Maxwell}}$  exerted on the oppositely charged plate:

$$\sigma_{\text{Maxwell}} = -\rho_s E_{\text{plate}} = -\frac{1}{2}\epsilon E_{\text{total}}^2 \quad (2.8)$$

This stress is termed *Maxwell stress*, and a rigorous derivation of the full tensor can be found in Reference [17].

The important point to take away is that the Maxwell stress between two oppositely charged parallel plates is always attractive and proportional to the electric field squared. Thus, if there is an insulator between the plates, then it will always experience compressive second-order stress due to squeezing from the plates. However, as mentioned in the previous section, all crystal classes exhibit electrostriction. Thus, contributions to second-order strain from Maxwell stress and electrostriction are ambiguous. Since it is difficult to separate the two contributions during measurement, **Maxwell stress is typically absorbed into the electrostriction coefficient** [16]. Thus, if a material is reported to have a positive electrostriction coefficient, then that material will expand at high electric fields with compressive Maxwell stress already taken into account.

## 2.5 Thermodynamics of Electroelastic Materials

In studying piezoelectric negative capacitance, we are essentially trying to analyze electromechanical positive feedback mechanisms and the work needed to execute them effectively. Thus, it is helpful to define and use appropriate free energies that allow us to understand the amount of energy available for work in our system. To begin, if we consider the intensive and extensive variables of typical elastic and electrical conjugate pairs, then we can easily construct the standard energy density differential for electroelastic materials

$$\partial u = \underbrace{\sigma_{ij} \partial \varepsilon_{ij}}_{\text{elastic energy density}} + \underbrace{E_i \partial D_i}_{\text{electric energy density}} + T \partial s \quad (2.9)$$

where  $T$  is temperature, and  $s$  is entropy density. Keep in mind that  $u$  is energy *density*. A total energy differential can be used instead by simply integrating Equation 2.9 over the volume of the material:

$$\partial U = \int_{\text{Volume}} \partial u \, dx dy dz \quad (2.10)$$

This will transform the conjugate variables accordingly such that stress and strain become force and displacement respectively; and electric field and electric displacement field become voltage and charge respectively.

Next, we can perform Legendre transformations to define various free energies for use with different control variables. This also determines the conditions under which each free energy has extrema. For example, the *electric Gibbs free energy density* [15] is defined as

$$g_{\text{electric}} = f - E_i D_i \quad (2.11)$$

where  $f = u - Ts$  is the Helmholtz free energy density. If we examine the corresponding exact differential,

$$\partial g_{\text{electric}} = \sigma_{ij} \partial \varepsilon_{ij} - D_i \partial E_i - s \partial T \quad (2.12)$$

then we can see that the electric Gibbs free energy density has extrema for a material allowed to freely strain (i.e. stress free) under constant electric field and isothermal conditions. If Equation 2.10 is used, then the electric Gibbs free energy [15] becomes

$$G_{\text{electric}} = F - QV \quad (2.13)$$

where  $F = U - TS$  is the Helmholtz free energy and  $S$  is entropy. The corresponding exact differential is given by

$$\partial G_{\text{electric}} = F_i \partial r_i - Q \partial V - S \partial T \quad (2.14)$$

where  $F_i$  and  $r_i$  are force and displacement respectively. This reveals that the total electric Gibbs free energy has extrema for a material allowed to freely strain under constant voltage and isothermal conditions. Thus, using the total free energy (Equation 2.13) can be more useful than using just the free energy density (Equation 2.11) when considering systems in which only the voltage can be easily controlled rather than the electric field. An example of such a system is a piezoelectric capacitor in which the electric field and piezoelectric thickness are coupled. Note that under isothermal conditions, the electric Gibbs free energy no longer depends on temperature or entropy. If temperature considerations are dropped altogether, then the electric Gibbs free energy collapses to *electric enthalpy*  $H_{\text{electric}}$  [15] and can be written more simply as

$$G_{\text{electric}} = H_{\text{electric}} = U - QV$$

where the internal energy  $U$  also no longer considers temperature.

We can also derive state equations from the free energies by using the corresponding exact differentials. For example, an expression for charge as a function of voltage can be derived from the electric Gibbs free energy by solving the following equation:

$$\left( \frac{\partial G_{\text{electric}}}{\partial Q} \right)_{\sigma_{ij}=0, V, T} = 0$$

The subscripts  $V$  and  $T$  denote constant voltage and constant temperature respectively. This simply follows our earlier statement that the electric Gibbs free energy has extrema for materials allowed to freely strain under constant voltage and isothermal conditions. For more information on electroelastic theory, please refer to Reference [15].

# 3

## Thermodynamic Model

### 3.1 Setup

In order for piezoelectricity to provide a negative capacitance effect, we learned in Section 2.1 that there must exist a positive feedback mechanism exploiting piezoelectricity. A simple system that implements such a mechanism is a capacitor with a piezoelectric insulator as shown in Figure 3.1. Jana et al. have also reported a similar system for achieving an electromechanical positive feedback mechanism [18].

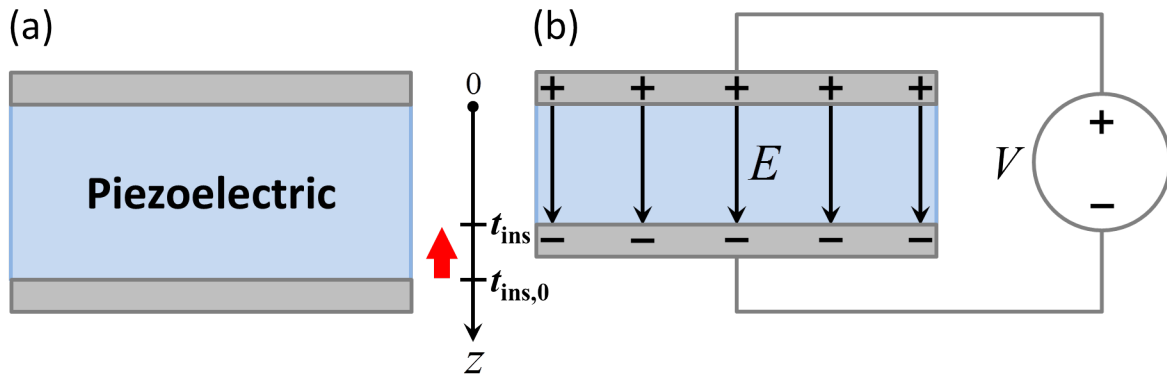


**Figure 3.1.** (a) A capacitor with a piezoelectric insulator of thickness  $t_{ins,0}$ . (b) Applying a voltage establishes an electric field that compressively strains the piezoelectric to a smaller thickness  $t_{ins}$  via the piezoelectric effect. The thinner piezoelectric results in a higher electric field for the same applied voltage. A higher electric field further compresses the piezoelectric, resulting in a compressive positive feedback mechanism. [12]

If we apply a voltage  $V$  to the capacitor shown in Figure 3.1a, then the capacitor will store some charge, resulting in an electric field  $E$  developing across the piezoelectric. From Section 2.2, we know that a piezoelectric material will linearly strain with electric field to first order. Thus, if we assume that the piezoelectric compresses for an electric field applied in the direction depicted in Figure 3.1b, then the capacitance will increase due to the thinner insulator. A higher capacitance will result in more charge stored for the same applied voltage. Thus, the electric field will become stronger and result in further compression via the piezoelectric effect. This process will continue to repeat, providing us with the electromechanical positive feedback mechanism necessary for achieving piezoelectric negative capacitance.

## 3.2 Model and Simulation

To model the proposed piezoelectric capacitor system, we used a thermodynamic framework that includes Equations 2.9, 2.10, and 2.13. These equations are repeated here for convenience:

$$\begin{aligned}\partial u &= \sigma_{ij} \partial \varepsilon_{ij} + E_i \partial D_i \\ \partial U &= \int_{\text{Volume}} \partial u \, dx dy dz \\ G &= U - QV\end{aligned}$$

Using this thermodynamic approach allowed us to conveniently analyze the negative capacitance effect in the presence of piezoelectricity, electrostriction, and ferroelectricity by simply including the corresponding energy terms in the internal energy. Note that these equations do not include temperature considerations because we are using the electric Gibbs free energy assuming isothermal conditions (see Section 2.5). Since strain contributions from Maxwell stress and electrostriction are indistinguishable (Section 2.4), it is inappropriate to treat Maxwell stress as a form of mechanical stress. As a result, we also assumed that our system was mechanically free (i.e.  $\sigma_{ij} = 0$ ). Under these assumptions, the electric Gibbs free energy differential simplifies to the following result:

$$\partial G = -Q \partial V \implies (\partial G)_V = 0$$

Thus, the electric Gibbs free energy has extrema under constant applied voltage.

To simulate the system, we swept the voltage and computed the electric Gibbs free energy as a function of charge for each applied voltage. We then searched for extrema in the resultant energy landscapes to find stable and unstable operating points. By doing this for enough voltage points, we were able to map out the operating behavior of the system and locate any regions of negative capacitance. The piezoelectric used in our simulations was modeled after 50 nm thick 52/48 lead-zirconate-titanate (PZT) because it is considered a strong piezoelectric and ferroelectric. The material parameters were chosen based on data from References [13, 19–22].

# 4

## Results

Note: The following results were previously published in my paper “Can piezoelectricity lead to negative capacitance?” [12].

### 4.1 Piezoelectric Negative Capacitance

The electric Gibbs free energy for a piezoelectric modeled after 52/48 PZT is shown in Figure 4.1 for different applied voltages:

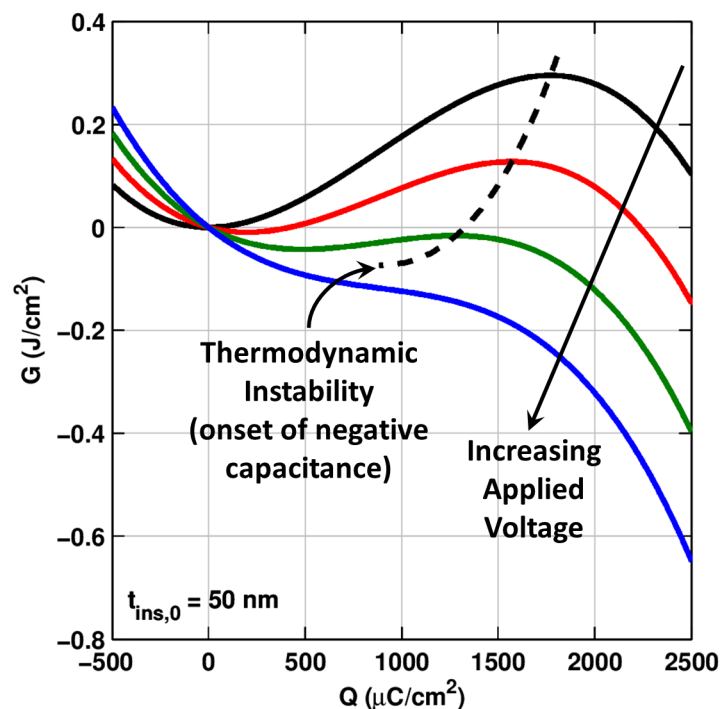
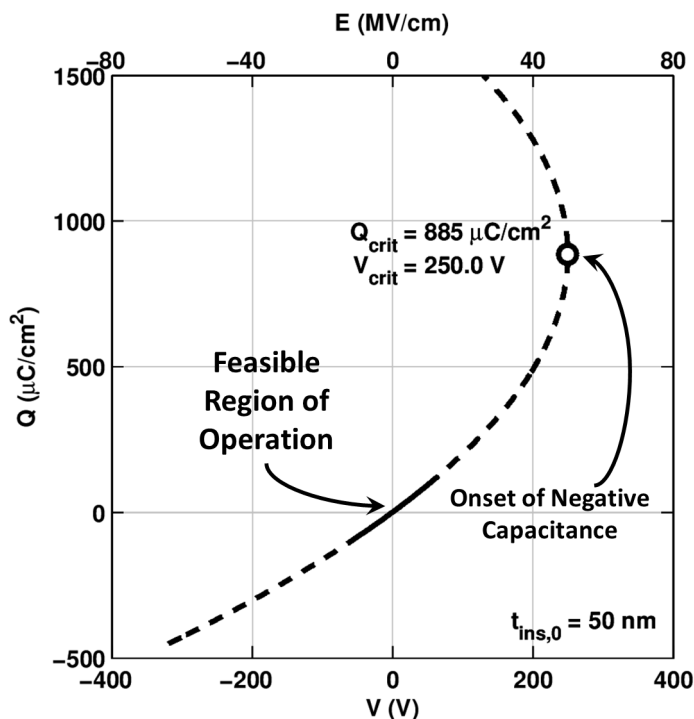


Figure 4.1. Electric Gibbs free energy for PZT under different applied voltages [12].

The solid black line shows the energy landscape under zero applied voltage, and the energy minimum at zero charge represents the stable operating point of the system. Notice, however, that

there is also an energy maximum at positive charge; this maximum indicates a thermodynamic instability and marks the onset of negative capacitance. When we increase the applied voltage, the energy landscape tilts as shown by the red and green lines. As this happens, the thermodynamic instability moves along the dashed black line, and the energy minimum and maximum approach each other. Thus, when a sufficiently high voltage is applied as shown by the blue line, the energy landscape no longer has any minima or maxima, and the system becomes unstable. At this point, the piezoelectric positive feedback mechanism described in Section 3.1 becomes strong enough to provide a negative capacitance effect.

Using the free energy computed in Figure 4.1, we can extract the charge stored in the system to obtain the  $Q$ - $V$  plot shown in Figure 4.2:



**Figure 4.2.** Charge versus voltage for the system thermodynamically analyzed in Figure 4.1. Negative capacitance is predicted to occur at an unphysical amount of charge and electric field [12].

The solid black line indicates the “feasible region of operation”, which we define as the region in which electric field intensity is nominally within 10 MV/cm. Most commonly used oxides have breakdown electric fields on the order of megavolts per centimeter, so trying to operate at an electric field of 10 MV/cm is already optimistic. Notice that while negative capacitance is predicted to occur as expected, it occurs at an unphysical amount of charge and electric field on the order of almost  $1000 \mu\text{C}/\text{cm}^2$  and tens of MV/cm respectively. This is clearly far outside the feasible region of operation. If we examine the strain in the system, we see a similar result as shown in Figure 4.3:

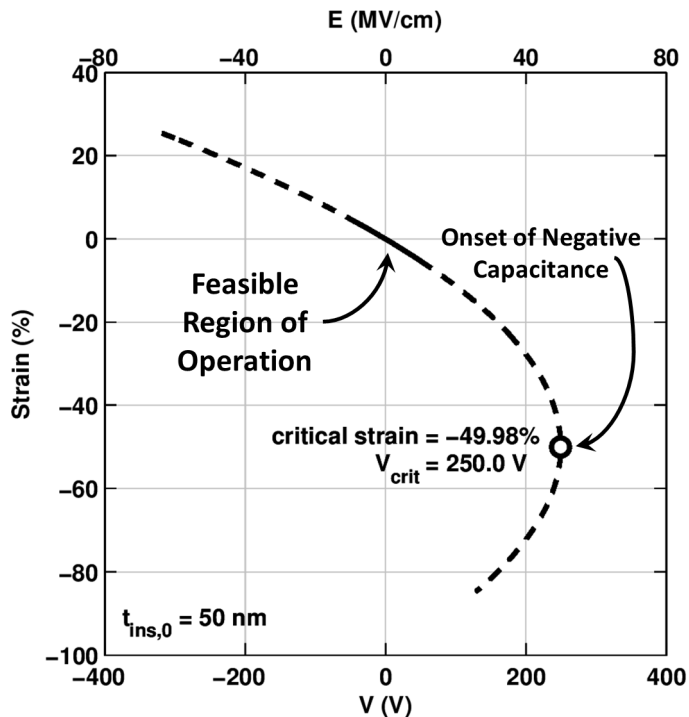


**Figure 4.3.** Strain versus voltage for the system thermodynamically analyzed in Figure 4.1. Negative capacitance is predicted to occur at an unphysical amount of strain and electric field [12].

Just as in the  $Q$ - $V$  plot, negative capacitance is predicted to occur but at an unphysical amount of strain on the order of tens of percent. **Clearly, piezoelectricity alone is not strong enough to access the negative capacitance region even in a strong piezoelectric such as 52/48 PZT.**

## 4.2 Incorporating Electrostriction

Since negative capacitance is predicted to occur at such high amounts of charge and electric field, it is insufficient to only consider piezoelectricity or *linear* electromechanical coupling. We need to take into account higher-order electromechanical coupling. As a result, we incorporated electrostriction into our model using PZT's electrostriction coefficient. The resultant electric Gibbs free energy is shown in Figure 4.4:

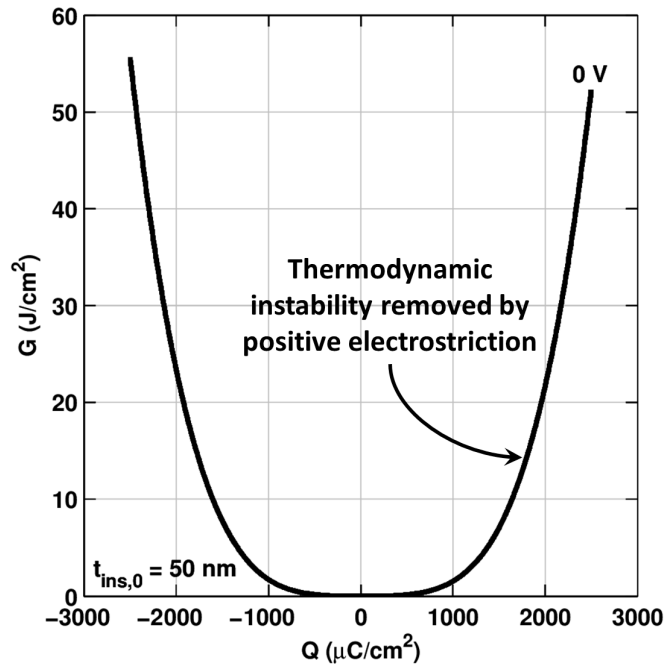


**Figure 4.4.** Electric Gibbs free energy under zero voltage for PZT with electrostriction taken into account [12].

The thermodynamic instability has been removed! This is due to the fact that PZT has a *positive* electrostriction coefficient—it expands at high electric fields. This expansion suppresses the compressive positive feedback mechanism needed to achieve negative capacitance. If we examine the charge stored in the system, then we obtain the  $Q$ - $V$  plot shown in Figure 4.5:

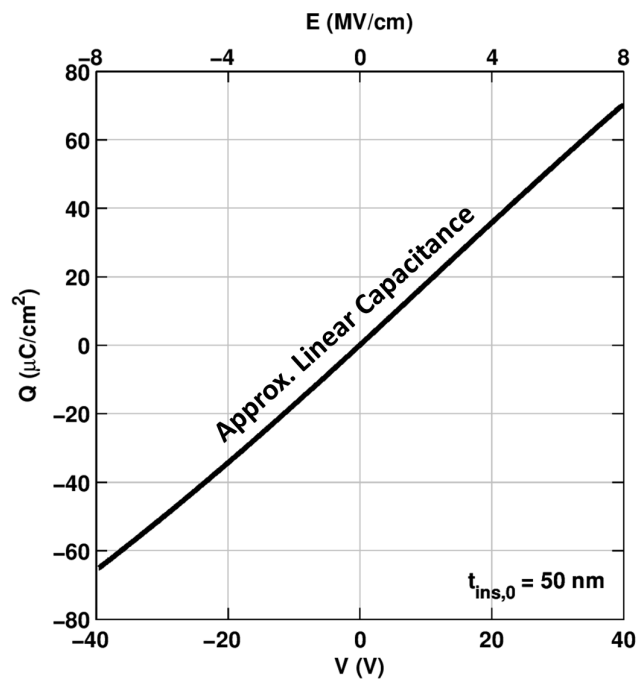


**Figure 4.5.** Charge versus voltage plotted for PZT with electrostriction taken into account. The negative capacitance region has been removed by positive electrostriction [12].

Notice that the capacitance has become linear with no signs of a negative capacitance region. If we also examine the strain in the system, then we obtain the plot shown in Figure 4.6:

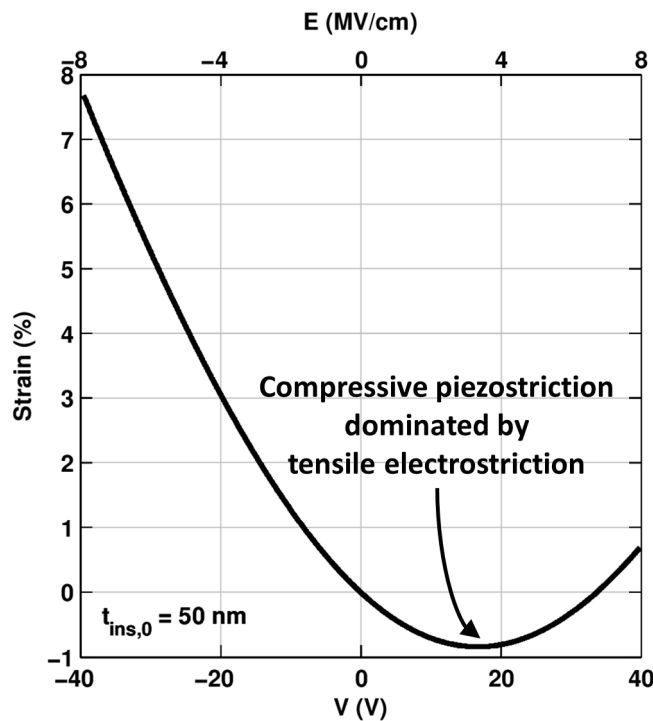


**Figure 4.6.** Strain versus voltage plotted for PZT with electrostriction taken into account [12].

The piezoelectric can only compress  $\sim 1\%$  via the piezoelectric effect before tensile electrostriction begins to dominate.

### 4.3 Tuning Electromechanical Negative Capacitance

Electrostriction clearly plays an important role in determining whether or not electromechanical negative capacitance can be achieved. In order to better understand this role, we chose different positive and negative electrostriction coefficients for PZT and computed the corresponding electric Gibbs free energies as shown in Figure 4.7:

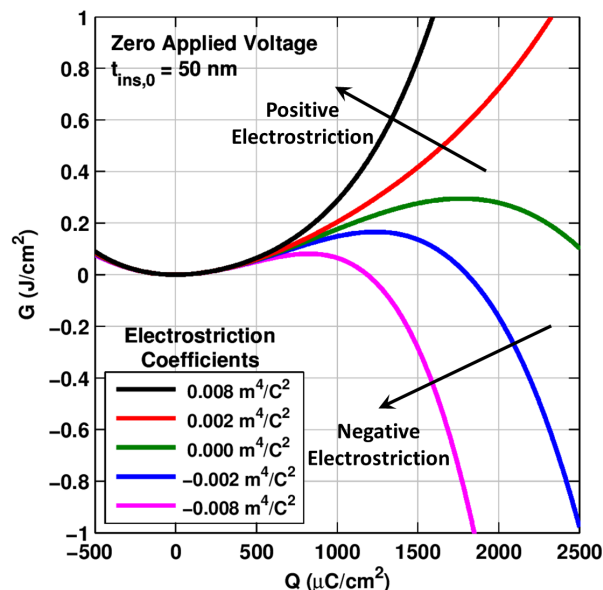


**Figure 4.7.** Electric Gibbs free energy under zero voltage computed for PZT using different positive and negative electrostriction coefficients. The thermodynamic instability is removed for positive electrostriction coefficients [12].

Notice that positive electrostriction removes the thermodynamic instability while negative electrostriction makes the instability easier to access with lower amounts of charge and electric field. **Consequently, oxides with positive electrostriction coefficients cannot exhibit electromechanical negative capacitance.** If we focus on increasingly negative electrostriction coefficients, then we can obtain the following plots of charge and strain:

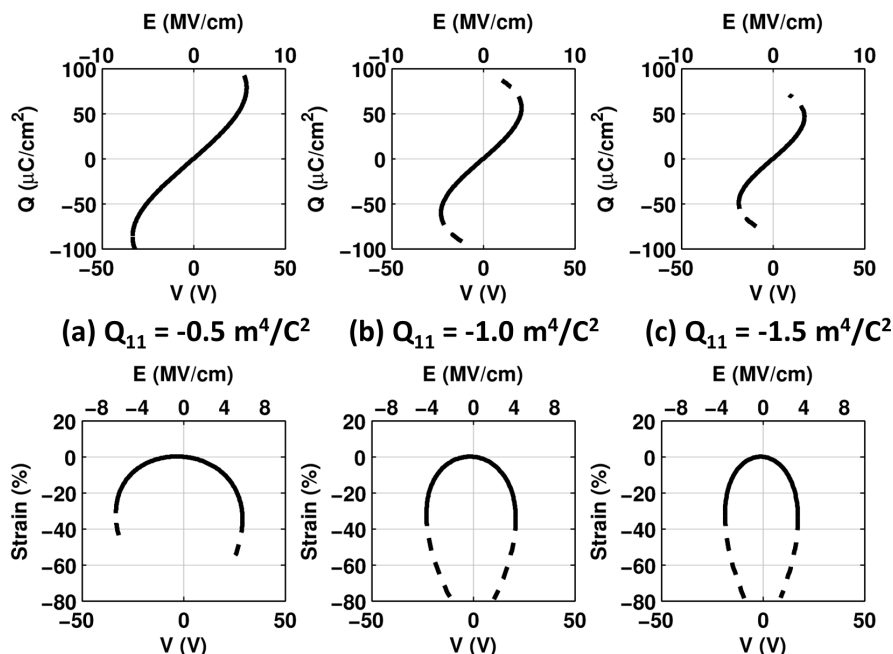


**Figure 4.8.** Charge and strain versus voltage for increasingly negative electrostriction coefficients from (a) to (c). The negative capacitance region becomes accessible at lower amounts of charge, but still requires unphysical amounts of strain [12].

The  $Q$ - $V$  plots in Figure 4.8 show that the critical amount of charge needed to access the negative capacitance region decreases with increasingly negative electrostriction coefficients. However, the strain plots reveal that the critical amount of strain is virtually unchanged and remains unphysical on the order of tens of percent. Let us now examine the actual electrostriction coefficients of commonly used oxides shown in Table I [16]:

TABLE I  
ELECTROSTRICTION COEFFICIENTS OF COMMON OXIDES

MATERIAL	ELECTROSTRICTION COEFFICIENT $Q_{11}$ ( $\text{m}^4/\text{C}^2$ )
BaTiO <sub>3</sub>	0.11
PbZr <sub>1-x</sub> Ti <sub>x</sub> O <sub>3</sub>	0.04 - 0.09
LiNbO <sub>3</sub>	0.016
LiTaO <sub>3</sub>	0.021
PMN-0.28PT	0.055
PMN-0.32PT	0.056
PMN-0.37PT	0.056
CaF <sub>2</sub>	-0.48
BaF <sub>2</sub>	-0.33
SrF <sub>2</sub>	-0.33

Unfortunately, we find that **most commonly used oxides have positive electrostriction coefficients and cannot exhibit electromechanical negative capacitance**. The fluorides do possess negative electrostriction coefficients, but their coefficients are not negative enough based on the results in Figure 4.8. Furthermore, they would still need to strain tens of percent.

## 4.4 Negative Capacitance in PZT

Finally, since PZT is actually a ferroelectric, we decided to take into account its complete ferroelectric properties. The resultant  $Q$ - $V$  plot is shown in Figure 4.9:

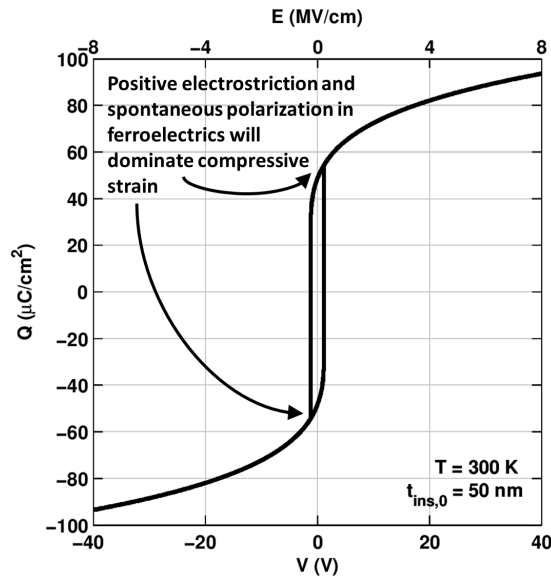


**Figure 4.9.** Charge versus voltage plotted for PZT with electrostriction and ferroelectricity taken into account [12].

We see a negative capacitance effect but due to the spontaneous polarization switching and not due to piezoelectricity. In addition, notice that the spontaneous polarization combined with positive electrostriction will result in a tendency for PZT to expand. We can understand this more clearly by examining the strain plot shown in Figure 4.10:

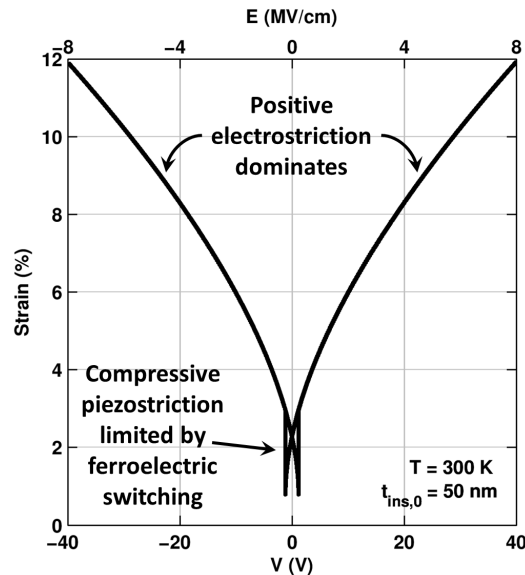


**Figure 4.10.** Strain versus voltage plotted for PZT with electrostriction and ferroelectricity taken into account [12].

As an electric field is applied in the opposite direction of the polarization, the material will compress a small amount via piezoelectricity before the polarization switches and the material begins to expand again. **Thus, when the full ferroelectric properties of PZT are included into our model, we see a negative capacitance effect but due to ferroelectricity and not piezoelectricity.**

# 5

## Conclusion

In conclusion, we showed that while piezoelectricity can provide a negative capacitance effect in principle, it is not strong enough in practice and requires unphysical amounts of charge and strain. If we include higher-order electromechanical coupling such as electrostriction, then the effect can become accessible with less charge but still requires strain on the order of tens of percent. Furthermore, most commonly used oxides have positive electrostriction coefficients, and, therefore, tend to expand rather than compress under high electric fields. This tendency suppresses the compressive positive feedback mechanism needed to achieve negative capacitance. Finally, when piezoelectricity, electrostriction, and ferroelectricity are analyzed together in a coherent platform, we observe a negative capacitance effect but due to ferroelectricity and not piezoelectricity. Thus, we conclude that for all practical purposes, pure electromechanical coupling is not strong enough to provide a negative capacitance effect.

# References

- [1] S. Agarwal and E. Yablonovitch, “Pronounced Effect of pn-Junction Dimensionality on Tunnel Switch Sharpness,” in *2013 Third Symposium on Energy Efficient Electronic Systems (E3S)*, 2013, pp. 1–2.
- [2] S. Salahuddin and S. Datta, “Use of Negative Capacitance to Provide Voltage Amplification for Low Power Nanoscale Devices,” *Nano Letters*, vol. 8, no. 2, pp. 405–410, Feb. 2008.
- [3] A. Rusu, G. A. Salvatore, D. Jimenez, and A. M. Ionescu, “Metal-Ferroelectric-Meta-Oxide-semiconductor field effect transistor with sub-60mV/decade subthreshold swing and internal voltage amplification,” in *2010 International Electron Devices Meeting*. IEEE, 2010.
- [4] A. I. Khan, D. Bhowmik, P. Yu, S. Joo Kim, X. Pan, R. Ramesh, and S. Salahuddin, “Experimental evidence of ferroelectric negative capacitance in nanoscale heterostructures,” *Applied Physics Letters*, vol. 99, no. 11, p. 113501, Mar. 2011.
- [5] M. H. Lee, J.-C. Lin, Y.-T. Wei, C.-W. Chen, W.-H. Tu, H.-K. Zhuang, and M. Tang, “Ferroelectric negative capacitance hetero-tunnel field-effect-transistors with internal voltage amplification,” *2013 IEEE International Electron Devices Meeting*, pp. 4.5.1–4.5.4, 2013.
- [6] A. I. Khan, K. Chatterjee, B. Wang, S. Drapcho, L. You, C. Serrao, S. R. Bakaul, R. Ramesh, and S. Salahuddin, “Negative capacitance in a ferroelectric capacitor,” *Nature Materials*, vol. 14, no. February, pp. 3–7, 2014.
- [7] W. Gao, A. Khan, X. Marti, C. Nelson, C. Serrao, J. Ravichandran, R. Ramesh, and S. Salahuddin, “Room-temperature negative capacitance in a ferroelectric-dielectric superlattice heterostructure.” *Nano letters*, vol. 14, no. 10, pp. 5814–9, Oct. 2014.
- [8] C. H. Cheng and A. Chin, “Low-Voltage Steep Turn-On pMOSFET Using Ferroelectric High-k Gate Dielectric,” *IEEE Electron Device Letters*, vol. 35, no. 2, pp. 274–276, Feb. 2014.
- [9] D. J. R. Appleby, N. K. Ponon, K. S. K. Kwa, B. Zou, P. K. Petrov, T. Wang, N. M. Alford, and A. O’Neill, “Experimental observation of negative capacitance in ferroelectrics at room temperature.” *Nano Letters*, vol. 14, no. 7, pp. 3864–8, Jul. 2014.
- [10] N. W. Ashcroft and N. D. Mermin, *Solid State Physics*. Cengage Learning, 1976.
- [11] H. W. Then, S. Dasgupta, M. Radosavljevic, L. Chow, B. Chu-Kung, G. Dewey, S. Gardner, X. Gao, J. Kavalieros, N. Mukherjee, M. Metz, M. Oliver, R. Pillarisetty, V. Rao, S. H. Sung, G. Yang, and R. Chau, “Experimental observation and physics of negative capacitance and

- steeper than 40mV/decade subthreshold swing in  $\text{Al}_{0.83}\text{In}_{0.17}\text{N}/\text{AlN}/\text{GaN}$  MOS-HEMT on SiC substrate,” in *2013 IEEE International Electron Devices Meeting*, vol. 117, no. 2004. IEEE, Dec. 2013, pp. 28.3.1–28.3.4.
- [12] J. C. Wong and S. Salahuddin, “Can piezoelectricity lead to negative capacitance?” in *2014 IEEE International Electron Devices Meeting*, 2014, pp. 13.5.1–13.5.4.
- [13] K. M. Rabe, C. H. Ahn, and J.-M. Triscone, *Physics of Ferroelectrics: A Modern Perspective*. Springer, 2007.
- [14] J. Tichý, J. Erhart, E. Kittinger, and J. Přivratská, *Fundamentals of Piezoelectric Sensors: Mechanical, Dielectric, and Thermodynamical Properties of Piezoelectric Materials*. Springer, 2010.
- [15] Z.-B. Kuang, *Theory of Electroelasticity*. Springer, 2014.
- [16] F. Li, L. Jin, Z. Xu, and S. Zhang, “Electrostrictive effect in ferroelectrics: An alternative approach to improve piezoelectricity,” *Applied Physics Reviews*, vol. 1, no. 1, p. 011103, Mar. 2014.
- [17] L. D. Landau and E. M. Lifshitz, *Electrodynamics of Continuous Media*. Pergamon Press, 1984.
- [18] R. K. Jana, G. L. Snider, and D. Jena, “On the possibility of sub 60 mV/decade subthreshold switching in piezoelectric gate barrier transistors,” *physica status solidi (c)*, vol. 10, no. 11, pp. 1469–1472, Nov. 2013.
- [19] V. Nagarajan, J. Junquera, J. Q. He, C. L. Jia, R. Waser, K. Lee, Y. K. Kim, S. Baik, T. Zhao, R. Ramesh, P. Ghosez, and K. M. Rabe, “Scaling of structure and electrical properties in ultrathin epitaxial ferroelectric heterostructures,” *Journal of Applied Physics*, vol. 100, no. 5, p. 051609, 2006.
- [20] Y. Bastani, T. Schmitz-Kempen, A. Roelofs, and N. Bassiri-Gharb, “Critical thickness for extrinsic contributions to the dielectric and piezoelectric response in lead zirconate titanate ultrathin films,” *Journal of Applied Physics*, vol. 109, no. 1, p. 014115, 2011.
- [21] H. Nazeer, M. D. Nguyen, L. a. Woldering, L. Abelmann, G. Rijnders, and M. C. Elwenspoek, “Determination of the Young’s modulus of pulsed laser deposited epitaxial PZT thin films,” *Journal of Micromechanics and Microengineering*, vol. 21, no. 7, p. 074008, Jul. 2011.
- [22] S. Zhong, S. P. Alpay, and V. Nagarajan, “Piezoelectric and dielectric tunabilities of ultra-thin ferroelectric heterostructures,” *Journal of Materials Research*, vol. 21, no. 06, pp. 1600–1606, Mar. 2011.